JACS
JOURNAL OF THE AMERICAN CHEMICAL SOCIETY

Article

Upgraded Bioelectrocatalytic N2 Fixation: From N2 to Chiral Amine Intermediates

Hui Chen, Rong Cai, Janki Patel, Fangyuan Dong, Hsiaonung Chen, and Shelley D. Minteer

J. Am. Chem. Soc., **Just Accepted Manuscript** • DOI: 10.1021/jacs.9b00147 • Publication Date (Web): 05 Mar 2019

Just Accepted

ACS Publications

is published by the American Chemical Society. 1155 Sixteenth Street N.W., Washington, DC 20036

Upgraded Bioelectrocatalytic N_2 Fixation: From N_2 to Chiral Amine Intermediates

Hui Chen,[†] Rong Cai,[†] Janki Patel,[†] Fangyuan Dong,[†] Hsiaonung Chen,[†] and Shelley D. Minteer[*,†]

[†] Departments of Chemistry and Materials Science & Engineering, University of Utah, 315 South 1400 East, RM 2020, Salt Lake City, Utah 84010, United States

* Corresponding Author: Shelley D. Minteer (minteer@chem.utah.edu)

KEYWORDS: N_2 fixation, Bioelectrocatalysis, Multi-enzyme cascade, Chiral amine chemical, Coenzyme regeneration

ABSTRACT: Enantiomerically pure chiral amines are of increasing value in the preparation of bioactive compounds, pharmaceuticals, and agrochemicals. ω-transaminase (ω-TA) is an ideal catalyst for the asymmetric amination as its excellent enantioselectivity and wide substrate scope. To shift the equilibrium of reactions catalyzed by ω-TA to the side of amine product, an upgraded N_2 fixation system based on bioelectrocatalysis was developed to realize the conversion from N_2 to chiral amine intermediates. The produced NH_3 was *in situ* reacted by *L*-alanine dehydrogenase to perform the alanine generation with NADH as a coenzyme. ω-TA transferred the amino group from alanine to ketone substrates and finally produced desired chiral amine intermediates. The cathode of the upgraded N_2 fixation system supplied enough reducing power to synchronously realize the regeneration of reduced methyl viologen ($MV^{\cdot+}$) and NADH for the nitrogenase and *L*-alanine dehydrogenase. The co-product, pyruvate, was consumed by *L*-alanine dehydrogenase to regenerate alanine and push the equilibrium to the side of amine. After 10 hours of reaction, the concentration of 1-methyl-3-phenylpropylamine achieved 0.54 mM with the 27.6% highest faradaic efficiency and >99% enantiomeric excess (ee_p). Due to the wide substrate scope and excellent enantioselectivity of ω-TA, the upgraded N_2 fixation system has great potential to produce a variety of chiral amine intermediates for pharmaceuticals and other applications.

INTRODUCTION

Enantiomerically pure chiral amines are of increasing value in organic synthesis.[1] There is an increasing demand for enantiomerically pure chiral amines, which are pivotal building blocks for the development of biologically active compounds including pharmaceuticals and agrochemicals.[1-2] ω-transaminase (ω-TA) has been a particular focus for research, because this enzyme offers a green route for the reductive amination of prochiral ketones to produce amines with high optical purity.[3] The challenge in asymmetric syntheses that employ ω-TA is to shift the equilibrium to the amine product side, especially when using an amino acid like alanine as a source of exogenous amine.[4-5] In this case, the equilibrium is on the side of the substrates (ketone and alanine) and not on the side of the products (amine and pyruvate).[6] In order to address this tricky problem, an alanine recycling method was established to remove pyruvate (co-product), regenerate the alanine and finally shift the reaction equilibrium to the side of amine products.[2, 7-8]

This alanine recycling reaction catalyzed by *L*-alanine dehydrogenase consumes NADH and ammonia (NH_3). Therefore, the regeneration of NADH and the supply of NH_3 are critical to carrying out this reaction. The traditional method for coenzyme regeneration is the addition of extra enzymes, such as formate dehydrogenase, NADH oxidase, alcohol dehydrogenase, phosphate dehydrogenase, glucose dehydrogenase, and corresponding co-substrates. Through the oxidation of auxiliary co-substrate, the cofactors can be regenerated.[9-10] Compared to chemical or enzyme-coupled coenzyme regeneration, bioelectrocatalytic regeneration methods get rid of the side products from the coenzyme as well as the substrate separation as the electricity can be the direct electron source for coenzyme regeneration and no by-product is produced.[11-12] Recently, the application of bioelectrocatalytic coenzyme regeneration for the synthesis of the desired chemical compound has gained prominence, due to the merits of utilizing clean electricity as a power source and highly selective enzymes as the catalyst while minimizing byproduct or pollutant formation.[13-14] Specifically, the bioelectrocatalytic coenzyme regeneration method has been used in the reaction for artificial photosynthesis,[15] the electrosynthesis of value-added products,[16-19] the asymmetric reduction of ketones and aldehydes to produce chiral alcohols, and the asymmetric reductive amination to produce chiral amines.[20-21] For the supply of NH_3, there are two methods. The one, which has been used in previous research,[2, 7-8] is

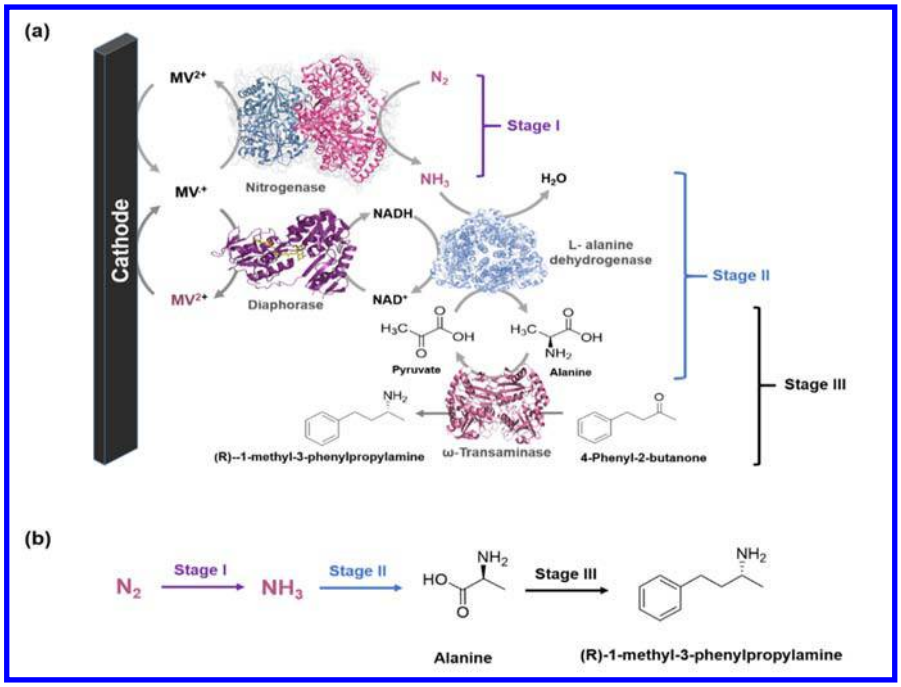

Figure 1. Schematic representation of the upgraded bioelectrocatalytic N_2 fixation system. (a) The components and the reaction process of the upgraded N_2 fixation system. (b) The conversion route from N_2 to chiral amine intermediate.

the direct addition of ammonium salts (NH_4Cl or $(NH_4)_2SO_4$) with high concentration. The other one, which is proposed herein, is to combine the alanine recycling with N_2 reduction and further to realize the *in situ* generation and utilization of NH_3. Recently, a novel mediated bioelectrocatalyitc N_2 fixation process based on nitrogenase has successfully been established by the Minteer group to realize N_2 reduction and NH_3 generation at ambient temperature and pressure.[22-23] The cathode could directly supply electrons to realize the effective regeneration of methyl viologen ($MV^{\cdot+}$) for the reduction of N_2 and NH_3 generation without adding any extra enzymes or co-substrates. Moreover, with the addition of diaphorase (DI), this bioelectrocatalysis system would also be able to perform the regeneration of NADH by using reduced $MV^{\cdot+}$ as reducing power. Consequently, it is feasible to combine the bioelectrocatalytic N_2 reduction and ω-TA catalyzed amination system to facilitate the preparation of chiral amines. Meanwhile, this combined system would be an upgraded N_2 fixation process as N_2 is ultimately converted to chiral amines but not NH_3.

During the past decades, chemists have sought economical methods of fixing atmospheric dinitrogen for use as fertilizers, explosives, and other chemicals.[24-26] The traditional Haber-Bosch process is an industrial process of N_2 fixation that produces NH_3 from molecular hydrogen (H_2) and molecular nitrogen (N_2) at the expense of >1% of global energy.[27] However, no matter the traditional Haber-Bosch process or the bioelectrocatalytic process mentioned above, the end-product of N_2 fixation is NH_3 which is a raw and commodity chemical. In the conversion from NH_3 to amines with complicated structures and higher added-value, tedious fine processing and the using of expensive transition metal catalysts are still required such as the palladium-catalyzed telomerization of butadiene and ammonia giving primary alkylamines, Pd-catalyzed allylic amination, copper and palladium catalyzed coupling reaction of ammonia with aryl halides to form arylamines, rhodium- and iridium-catalyzed reductive aminations of carbonyl compounds with ammonium formate and ammonia to afford primary alkylamines and palladium-catalyzed arylation of ammonia to afford di-and triarylamines.[28] Consequently, it is necessary to develop an upgraded N_2 fixation system. In this upgraded system, NH_3 would no longer be the end-product of N_2 fixation, but an intermediate that could be further *in situ* utilized to realize the one-pot synthesis of chemicals with more complicated structure and higher added-value without using the expensive transition metal catalysts.

In this study, we established an upgraded N_2 fixation system that contained a nitrogenase from *Azotobacter vinelandii* (EC1.18.6.1), a diaphorase (DI, EC1.6.99.3) from *Thermotaga maritima*, a *L*-alanine dehydrogenase from *Bacillus subtilis* (AlaDH, EC1.4.1.1) and a ω-TA originated from *Hyphomonas neptunium* (HN-ωTA, EC 2.6.1.18) to perform the conversion from N_2 to chiral amine intermediates (**Figure 1a**). In this upgraded N_2 fixation system, the cathode provided electrons to perform the effective regeneration of reduced $MV^{\cdot+}$ and NADH. Reduced $MV^{\cdot+}$ is the electron donor for NH_3 generation catalyzed by nitrogenase. The generated NH_3 was utilized *in situ* by AlaDH to realize the amination of pyruvate and the alanine generation with the regenerated NADH as the coenzyme. HN-ωTA transferred the amino group from alanine to the ketone substrates and produced desired chiral amine chemicals. Ultimately, N_2 was converted to chiral amines through NH_3 and alanine (**Figure 1b**).

RESULTS AND DISCUSSION

Design and construction of the upgraded N_2 fixation system. An H-shaped dual-chamber bioelectrochemical reactor was used and separated by a proton exchange membrane (PEM). The protons generated at the platinum anode were able to pass through the PEM into the cathodic chamber. The electrons from the Toray carbon paper cathode were used to reduce the electron mediator, MV^{2+}, which was used to provide the reducing power for N_2 reduction and NADH regeneration.

The upgraded N_2 fixation process is composed of three stages (**Figure 1a**). Stage I is the bioelectrocatalytic N_2 reduction and NH_3 generation. In this stage, the N_2 is initially reduced to NH_3 which is catalyzed by nitrogenase in the existence of an ATP regeneration system (creatine phosphate, creatine phosphokinase, and ADP). The reduced $MV^{\cdot+}$ generated from the cathode was employed as the electron donor for NH_3 generation.[22] Stage II is the *in situ* NH_3 capture and the generation of alanine. In this stage, the NH_3 generated in stage I was captured by AlaDH to produce alanine by using pyruvate as the NH_3 acceptor and NADH as the reducing power. Furthermore, NADH can be recycled by DI and reduced $MV^{\cdot+}$ which was regenerated by the cathode. In the first two stages, The cathode in the bioelectrocatalytic system provided electrons for the synchronous regeneration of both reduced $MV^{\cdot+}$ and NADH. Compared to the traditional method, the bioelectrocatalytic coenzyme regeneration does not require the addition of extra oxidoreductase enzymes and their corresponding co-substrates. Electricity can be used instead of the oxidoreductase for cofactor regeneration. Also, no by-product is produced, which facilitates the recovery of the desired product as it does not require a co-substrate.[9-11] Stage III is the amino-group transfer and the generation of the chiral amine intermediate. In this stage, the alanine generated in stage II was employed as the source of exogenous amine and the amino group could be transferred to different ketone substrates and finally generate the corresponding chiral amine chemicals. As the equilibrium of the reaction catalyzed by HN-ωTA strongly favored the ketone/alanine side, rather than the amine/pyruvate side,[2, 5] shifting the ketone/amine equilibrium to favor the amine is a challenging task, especially when using alanine as the source of exogenous amine.[29-30] In the upgraded N_2 fixation system, the generated pyruvate is consumed by AlaDH to regenerate alanine by consuming NH_3 and NADH, which could push the equilibrium to the side of amine. The coenzyme, NADH, can also be recycled by DI and reduced $MV^{\cdot+}$. In this concept, alanine and NADH are not consumed, but recycled in the upgraded N_2 fixation system. The N_2 is converted to chiral amine chemicals via NH_3 and alanine (**Figure 1b**).

Bioelectrocatalysis using MV^{2+} as an electron mediator. Initial cyclic voltammetric (CV) (**Figure 2**) was used to demonstrate the ability of the cathode to act as the primary electron donor of nitrogenase and DI, where MV^{2+} serves as an electron mediator between the electrode and both nitrogenase and DI (**Figure 1a**).

The CV of 100 μM MV^{2+} revealed that oxidized MV^{2+} was reduced to $MV^{+\cdot}$ at approximately -0.75V vs. SCE. After the adding of 0.16 U/mL nitrogenase (0.2 mg/mL MoFe protein, a Fe:MoFe protein ratio of 16:1) and 6.7 mM $MgCl_2$ (to initiate protein turnover), a catalytic wave was observed corresponding to nitrogenase turnover at approximately -0.75 V vs SCE, which demonstrated the electron transfer from cathode to nitrogenase mediated by MV^{2+}. After the adding of 0.16 U/mL DI (0.04 mg/mL), and 100 μM NAD^+, a more obvious catalytic wave was observed at approximately -0.75 V vs. SCE corresponding to the additional reduction of NAD^+ on the basis of nitrogenase turnover. The reduced $MV^{\cdot+}$ generated from cathode was further utilized by DI as an electron donor to realize the generation of NADH. However, it is important to note that methyl viologen is a better mediator for nitrogenase than diaphorase. In order to maintain a high electron flow for the reaction, the working potential for the bioelectrocatalytic system was set at -0.85 V vs. SCE.

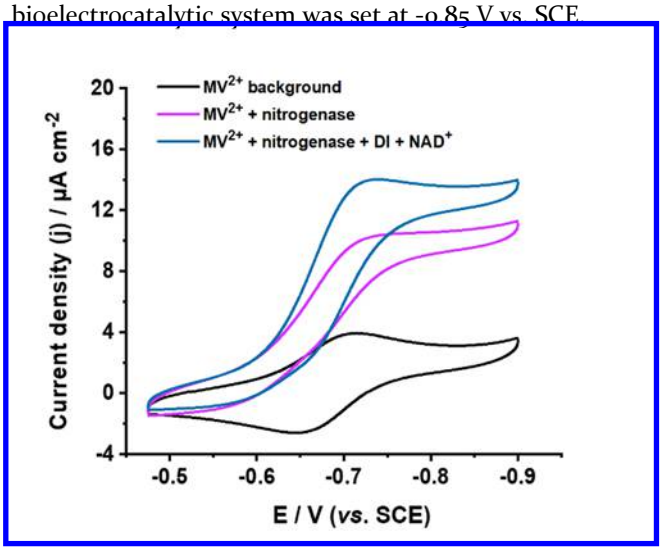

Figure 2. Representative cyclic voltammograms of nitrogenase bioelectrocatalysis mediated by MV^{2+} for N_2 reduction and the regeneration of NADH with the addition of DI. Black line: the current response of MV^{2+} background (100 μM MV^{2+} in ATP-regeneration solution which contained 100 mM MOPS, pH=7.0, 6.7 mM $MgCl_2$, 30 mM creatine phosphate, 5 mM ATP, 0.2 mg/mL creatine phosphokinase and 1.3 mg/mL bovine serum albumin); Orchid line: the current response of MV^{2+} background system supplemented with 0.16 U/mL nitrogenase (0.2 mg MoFe protein, MoFe protein: Fe protein = 1:16 by mole) and 6.7 mM $MgCl_2$ for N_2 reduction; Blue line: the current response of N_2 reduction system supplemented with 100 μM NAD^+ and 0.16 U/mL DI (0.04 mg/mL).

Amperometric *i*-t analysis of the upgraded N_2 fixation system. As NH_3 is the initial substrate of bioelectrosynthesis of 1-methyl-3-phenylpropylamine, the concentration of nitrogenase was first optimized to obtain as much NH_3 as possible (**Figure S2**). The result indicated that 0.16 U/mL (0.2 mg/mL) MoFe protein is the best concentration to achieve NH_3 concentrations as high as 1.4 mM.

After the optimization of nitrogenase concentration, the amperometric *i*-t analysis was used to analyze the reaction process. In the amperometric *i*-t curve (**Figure 3**), the entire reaction process was partitioned into three stages by two different injections. The initial stage is NH_3 generation catalyzed by nitrogenase with 750 μM MV^{2+} as the electron mediator. When the reaction achieved steady state (approximately 5 hours of reaction), the current stabilized. Upon the addition of 0.18 U/mL AlaDH, 0.16 U/mL DI, 200 μM NAD^+ and 50 μM pyruvate to the electrolyte, a dramatic increase in the reductive current of both the reactions with and without nitrogenase was observed. This response could be due to the reduction of NAD^+ catalyzed by DI with the consumption of reduced $MV^{\cdot+}$. After the current peaked, the current response of reaction with and without nitrogenase exhibited a different trend. For the reaction with nitrogenase, the reductive current decreased slowly. In contrast, the reductive current of the reaction without nitrogenase exhibited a dramatic decrease. It is speculated that the NH_3 generated by nitrogenase could be utilized by AlaDH to produce alanine with the consumption of pyruvate and NADH. The loading of nitrogenase, DI, and AlaDH is 0.16 U/mL, 0.16 U/mL and 0.18 U/mL respectively. As the enzyme activity units of the three enzymes are in balance and the rate of MV^{2+} reduction catalyzed by cathode is high enough (k_{obs} = 25/s at 30 °C),[31] the NADH and NH_3 consumed by AlaDH could be regenerated effectively. In order to regenerate NADH, oxidized MV^{2+} continuously obtained electrons from the cathode and finally kept the current at a higher level. In order to verify this hypothesis, UPLC-MS was employed to detect the alanine generation of the reactions with and without nitrogenase. The result of UPLC-MS (**Figure S3**) indicated that alanine was indeed generated in the reaction with nitrogenase. Oppositely, no alanine was generated in the reaction without nitrogenase.

Upon the addition of substrate, 2 mM 4-phenyl-2-butanone, a new peak in the reductive current was observed in the reaction with nitrogenase. This response could be due to the formation of the final product 1-methyl-3-phenylpropylamine accelerating the alanine recycling rate and coenzyme regeneration rate. The formation of product 1-methyl-3-phenylpropylamine in the reaction with nitrogenase was proven by GC-MS (**Figure S4**).

In this study, monitoring of the current can be used to monitor the progress of the reaction. Compared to the traditional reaction process analysis which was based on the formation of the intermediate and product, the reaction process analysis based on electrical signal has the advantages of speed, convenience, and high sensitivity. The cathode provided electrons for the synchronous regeneration of both reduced $MV^{\cdot+}$ and NADH and further effectively drives the N_2 reduction and pyruvate amination. The NH_3 generated from N_2 fixation was utilized by AlaDH to realize the regeneration of alanine by consuming pyruvate, pushing the equilibrium to the side of the product and ultimately producing the chiral amine products. Additionally, the generated NH_3 was captured by AlaDH to generate alanine. On this basis, it is feasible for the upgraded N_2 fixation system to employ other amino acid dehydrogenase such as leucine dehydrogenase. phenylalanine dehydrogenase and valine dehydrogenase to generate leucine,[32] phenylalanine [33] and valine.[34]

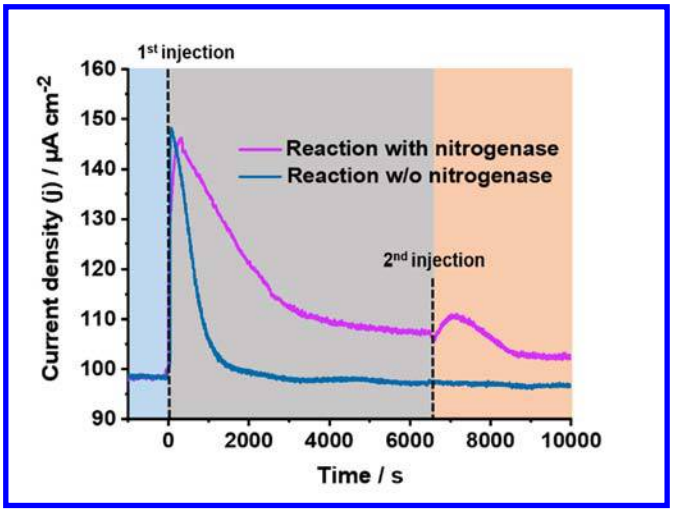

Figure 3. Amperometric *i*-t curve of the upgraded N_2 fixation system. The MV^{2+} (750 μM) mediated bioelectrocatalytic N_2 reduction by nitrogenase was sequentially supplemented with components of alanine (1st injection) and 1-methyl-3-phenylpropylamine (2nd injection) generation with (orchid line) and without (blue line) nitrogenase at 30 °C. The experiments were performed in an anaerobic H-shaped cell with stirring in N_2 reduction solution (3 mL, complete with the ATP-regeneration system), where the 0.16 U/mL nitrogenase (0.2 mg/mL of MoFe protein coupled with Fe protein at 1:16 ratio by mol) and the final $MgCl_2$ concentration was 6.7 mM. 0.1 U/mL dry *E. coli* cells (20 mg/mL) and 1 mM PLP were initially added. A constant potential -0.85 V *vs* SCE was employed at 30 °C. In the 1st injection, 0.18 U/mL AlaDH, 0.16 U/mL DI, 200 μM NAD^+ and 50 μM pyruvate was supplemented. In the 2nd injection, 2 mM 4-phenyl-2-butanone was supplemented.

Optimization of pyruvate concentration. The current response upon the addition of different pyruvate concentrations, which is a sensitive indicator of electron transfer and reaction rate, was measured by using amperometric *i*-t analysis. As shown in **Figure 4a**, the injection of pyruvate led to a rapid current response which meant the consumption of NADH for the generation of alanine accelerated the electron transfer from the cathode to NADH via reduced $MV^{\cdot+}$. Furthermore, the intensity of current response was determined by the injection concentration of pyruvate. From 10 μM to 50 μM, increasing the pyruvate injection concentration led to higher current response. Injection 50 μM pyruvate achieved the most significant current response which increased from approximately 100 μA/cm^{-2} to 160 μA/cm^{-2}. However, to continue increasing the injection concentration of pyruvate to 100 μM, the current response only increased from approximately 100 μA/cm^{-2} to 120 μA/cm^{-2}, which was almost the same with that of a 10 μM pyruvate injection concentration. Moreover, compared with 25 and 50 μM injection concentrations, the current

response of 10 and 100 μM injection concentration is falling faster. The concentration of the final product, 1-methyl-3-phenylpropylamine, has a direct relationship with the current response (**Figure 4b**). The concentration of the 1-methyl-3-phenylpropylamine product with 50 μM pyruvate injection was 0.54 mM, almost two times higher than that of 10 μM (0.26 mM) and 100 μM pyruvate injections (0.27 mM). The reaction with 25 μM pyruvate injection generated 0.36 mM 1-methyl-3-phenylpropylamine.

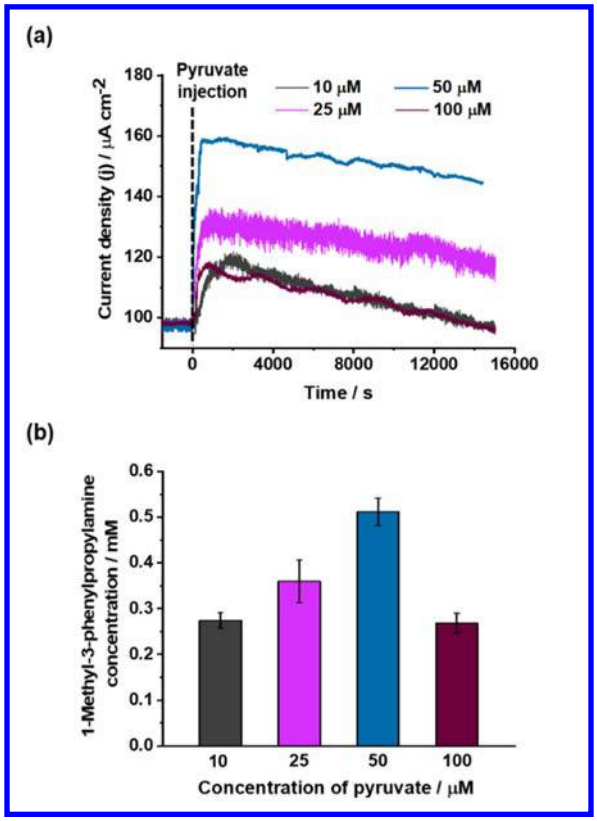

Figure 4. The optimization of pyruvate concentration. The reactions contain MOPS buffer (100 mM, pH = 7.0), MV^{2+} (750 μM), NAD^+ (200 μM), PLP (1 mM), 1-methyl-3-phenylpropylamine (2 mM) and pyruvate at different concentration. The reaction was performed by employing 0.16 U/mL nitrogenase, 0.18 U/mL AlaDH, 0.16 U/mL DI and 0.1 U/mL dry *E.coli* cell containing HN-ωTA. (a) Amperometric *i*-t curve of the current response on injection of pyruvate at different concentration using a constant potential of -0.85 V *vs.* SCE, (b) The concentration of 1-methyl-3-phenylpropylamine generated by the upgraded N_2 fixation process with different pyruvate concentrations.

The results demonstrated the important role of pyruvate concentration on the generation of amine product. The coproduct, pyruvate, must be removed to push the reaction equilibrium to the side of amine product and enhance the accumulation of amine. Meanwhile, pyruvate is the acceptor of NH_3 generated from N_2 reduction. Excessively low concentrations of pyruvate could decrease the efficiency of NH_3 capture and transfer. Therefore, the pyruvate concentration needs to be optimized to achieve the trade-off between accumulation and consumption. In this study, the current response has good consistency with the concentration of the final amine product. As current is proportional to the number of electrons transferred from the electrode to electron mediators,[35] the current density is the reflection of electron transfer rate, which directly correlated with the production rate of the final product. Consequently, the current response can be used as a sensitive indicator for reaction optimization. Compared to traditional reaction optimization which is based on the measurement of intermediator or product, using the current response as an indicator is a much faster and simpler way to screen the reaction conditions and the concentration of the substrate and the intermediate.

Bioelectrosynthetic 1-methyl-3-phenylpropylamine production. The concentration of 1-methyl-3-phenylpropylamine that was electroenzymatically synthesized in a H-shaped dual-chamber bioelectrochemical reactor with 2 mM 4-phenyl-2-butanone as the substrate as a function of time is shown in **Figure 5**. After 10 hours of reaction, the concentration of 1-methyl-3-phenylpropylamine achieved the highest level (approximately 0.54 mM). Continuous reaction to 12 hours did not increase the product concentration. The faradaic efficiency of the bioelectrocatalytic reaction was calculated as a function of time. Similar to the generation of 1-methyl-3-phenylpropylamine, the highest faradaic efficiency was observed during the 4th hour, which is approximately 27%. After 4 hours, the faradaic efficiency decreased gradually. When 1-methyl-3-phenylpropylamine achieved its highest concentration, the faradaic efficiency decreased to 16%.

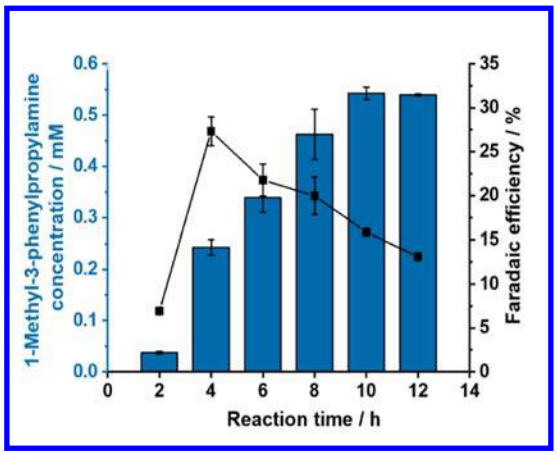

Figure 5. The concentration of 1-methyl-3-phenylpropylamine generated in the upgraded N_2 fixation system and corresponding faradaic efficiency following a 14 hour time course. The reactions contain MOPS buffer (100 mM, pH = 7.0), MV^{2+} (750 μM), NAD^+ (200 μM), PLP (1 mM), 1-methyl-3-phenylpropylamine (2 mM) and pyruvate (50 μM). The reaction was performed by employing 0.16 U/mL nitrogenase, 0.18 U/mL AlaDH, 0.16 U/mL DI and 0.1 U/mL dry *E.coli* cell containing HN-ωTA.

Bioelectrosynthetic reductive amination of substrates with different structures. Eight different prochiral ketones (**Figure 6**) were employed as an exogenous amine in the upgraded N_2 fixation system to produce corresponding the amines (**Figure S5**). After 10

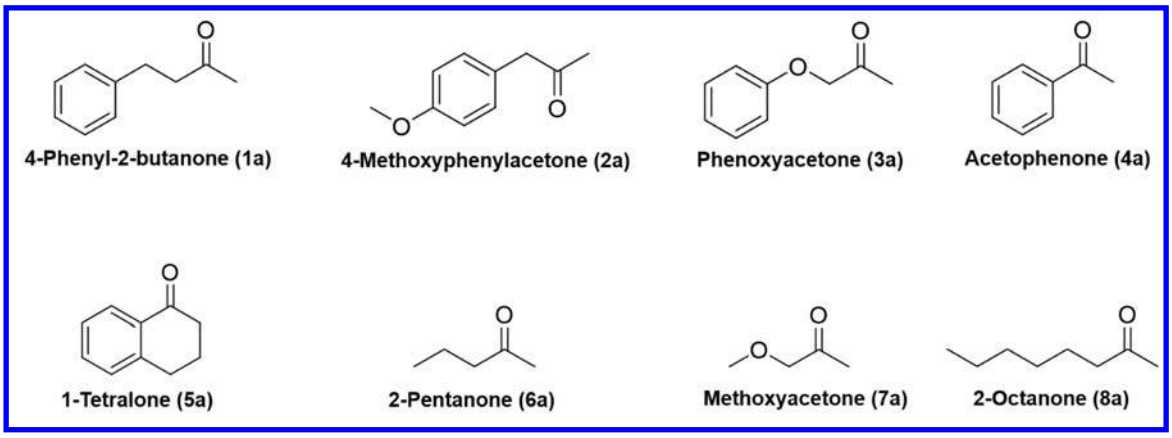

Figure 6. The prochiral ketones as the substrates of upgraded N_2 fixation system to produce chiral amines.

Table 1. Asymmetric amination of various prochiral ketones catalyzed by upgraded N_2 fixation system.

Entry	Substrate	Product concentration (mM)[a]	ee_p (%)[b]	Yield rate (mol·L^{-1}·h^{-1})
1	1a	0.54	>99 (R)	54
2	2a	0.34	>99(R)	34
3	3a	0.61	>99(R)	61
4	4a	nd[c]	n.d.[c](R)	n.d.
5	5a	nd[c]	n.d.[c](R)	n.d.
6	6a	0.14	>99(R)	14
7	7a	0.53	>99(R)	53
8	8a	0.35	>99(R)	35

Each value represents the means from triplicate experiments.
[a] The reactions contain MOPS buffer (100 mM, pH = 7.0), MV^{2+} (750 μM), NAD^+ (200 μM), PLP (1 mM), substrate (2 mM), pyruvate (50 μM), nitrogenase (0.16 U/mL), AlaDH (0.18 U/mL), DI (0.16 U/mL) and dry *E.coli* cell containing HN-ωTA (0.1 U/mL).
[b] In [%]. Determined by GC on a chiral stationary phase after derivatization to the corresponding acetamide.
[c] n.d. Not determined due to too low conversion

hours of reaction (**Table 1**), the HN-ωTA performed the amination of almost all of the substrates, except substrate 4a and 5a, with perfect stereoselectivity (>99% ee_p) to the corresponding (*R*)-amines. After 10 hours of reaction, the amination product of 3a achieved the highest concentration at 0.61 mM. The results are basically in accordance with previous reports,[8] which means the electrocatalytic system does not change the catalytic properties of HN-ωTA. From the wide substrate scope and excellent enantioselectivity, the N_2 could be fixed to a variety of chiral amine substrates with high ee_p. The obtained amine products are intermediates for various products.[8] For example, (*R*)-1b is a precursor of the antihypertensive dilevalol,[36-37] (*R*)-2b can be used to synthesize the bronchodilator formoterol.[38] and (*R*)-3b has the same backbone of the antiarrhythmic, antimyotonic and analgesic drug (*R*)-mexiletin.[39-40] antimyotonic and analgesic drug (*R*)-mexiletin.[39-40]

In the bioelectrocatalytic upgraded N_2 fixation system, the AlaDH,[41] DI,[42] HN-ωTA[8] as well as nitrogenase (**Figure S2**) are stable enough and work steadily at 30 °C. The generation of NH_3 catalyzed by nitrogenase is the initial step of the reaction pathway. Due to the low solubility of N_2,[43] the accumulation rate of ammonia is not high enough (1.4 mM after 10 hours of reaction). The N_2 reduction is the limiting step of the upgraded N_2 fixation system. Consequently, further improvement of nitrogenase activity and the accumulation rate of NH_3 were critical for increasing the catalytic efficiency of the upgraded N_2 fixation system. Compared with the traditional biocatalysis system of chiral amine production,[2, 7-8] the bioelectrocatalytic upgraded N2 system is a proof of concept. However, the bioelectrocatalytic upgraded N_2 fixation system exhibited an attractive possibility that the N_2 reduction could directly be converted to high value-added chemicals through one-pot multi-enzymatic bioelectrocatalysis with low energy consumption. Specifically, the chemically inert N_2 which forms the majority of the earth's atmosphere could be captured and reduced by nitrogenase, transferred to alanine by AlaDH and finally utilized by HN-ωTA to produce chiral amines. Consequently, the upgraded N_2 fixation system realized the comprehensive utilization of chemically inert dinitrogen. Additionally, due to the one-pot chiral amine production mode, the complicated multi-enzyme reaction could be performed in the same "pot" at mild condition without using expensive transition metal catalysts. This

flexible production mode has great potential to realize the distributed and green manufacture of chiral amines.

CONCLUSION

In summary, we present a novel upgraded N_2 fixation system based on a bioelectrocatalytic N_2 reduction system in which the end-product of N_2 fixation successfully surpassed NH_3 and reached high value-added chiral amine intermediates. From the wide substrate scope of ω-TA, our upgraded N_2 fixation system has the potential to generate a variety of chiral amine chemicals with different structures. This proof of concept still has the possibility of improvement such as the development of ATP-independent electroenzymatic reduction system of N_2 fixation. Some achievements have already been achieved by our group in removing the need for an ATP regeneration system,[44] as well as the industrial solution of immobilizing the mediator at the electrode surface for decreasing issues of toxicity and large quantities of mediator.

MATERIALS AND METHODS

Chemicals, bacterial strains, and medium. Unless stated otherwise, all chemicals were purchased from Sigma Aldrich. Saturated calomel reference electrodes (SCE) were purchased from CH Instruments, Inc. All bioelectrocatalytic experiments were performed at <1 ppm O_2 in an anaerobic tent (Coy Laboratory Products, MI, USA) or within septum-sealed vials. Synthetic gene fragments including the genes of AlaDH, DI and HN-ωTA were purchased from Genscript, Inc. *Azobobacter vinelandii* (ATCC® BAA-1303™) was purchased from the American Type Culture Collection. Oligonucleotides were synthesized by the DNA/Peptide Facility, part of the Health Sciences Cores at the University of Utah. Toray carbon paper (untreated) was purchased from Fuel Cell Earth (USA). All of the enzymes for molecular biology experiments were purchased from New England Biolabs (NEB, Ipswich, MA, USA). *E. coli* Top10 was used for general molecular cloning and *E. coli* BL21 (DE3) was used for recombinant protein expression. The Luria-Bertani (LB) medium was used for *E. coli* cell culture and recombinant protein expression. The final concentrations of antibiotics for *E. coli* were 100 mg/L ampicillin. *A. vinelandii* was cultured as reported using a modified Burk media: sucrose (58.4 mM), $MgSO_4$ (0.81 mM), $CaCl_2$ (0.61 mM), $FeCl_3$ (0.1 mM), Na_2MoO_4 (0.01 mM), NH_4OAc (when required, 10 mM), K_2HPO_4 (3.51 mM) and KH_2PO_4 (1.47 mM).[45]

Construction of plasmids. The strains and plasmids used in this study are summarized in **Table S1** and the sequences of all PCR primers used were listed in **Table S2**. All of the plasmid sequences were validated by DNA sequencing.

Plasmid pET20b-AlaDH had an expression cassette containing *L*-alanine dehydrogenase from *B. subtilis* (GenBank Accession number: L20916.1). The DNA sequence fragment was synthesized by Genescript (Piscataway, NJ, USA) and amplified by PCR using a pair of primers IF-AlaDH and IR-AlaDH; pET20b vector backbone was amplified with a primer pair of VF-AlaDH and VR-AlaDH. Plasmid pET20b-AlaDH based on two DNA fragments was obtained by using Simple Cloning.[46]

Plasmid pET20b-DI had an expression cassette containing diaphorase from *T. maritima* (GenBank Accession number: CP011108.1). The DNA sequence fragment was synthesized by Genescript (Piscataway, NJ, USA) and amplified by PCR using a pair of primers IF-DI and IR-DI; pET20b vector backbone was amplified with a primer pair of VF-DI and VR-DI. Plasmid pET20b-DI based on two DNA fragments was obtained by using Simple Cloning.[46]

Plasmid pET20b-HN-ωTA had an expression cassette containing HN-ωTA from *H. neptunium* (GenBank Accession number: ABI75539.1). The DNA sequence fragment was synthesized by Genescript (Piscataway, NJ, USA) and amplified by PCR using a pair of primers IF-ωTA and IR-ωTA; pET20b vector backbone was amplified with a primer pair of VF-ωTA and VR-ωTA. Plasmid pET20b-ωTA based on two DNA fragments was obtained by using Simple Cloning.[46]

Expression and purification of enzymes. The growth of *Azotobacter vinelandii* and the purification of nitrogenase protein was performed as previously described.[22]

The strains *E. coli* BL21(DE3) containing the protein expression plasmids of AlaDH and DI were cultivated in the LB medium supplemented with 1.2% glycerol at 37°C. When A_{600} reached about 0.8, 100 μM isopropyl-beta-D-thiogalactopyranoside (IPTG, a final concentration) was added and the cultivation temperature was decreased to 18 °C for ~16 hours. His-tagged proteins were purified as below. After induction with IPTG, cells were harvested by centrifugation. The cell pellets were re-suspended in 100 mM MOPS buffer (pH 7.0) containing and 50 mM NaCl. For the purification of DI, 0.1 mM flavin adenine dinucleotide (FAD) was added after ultrasonication. After centrifugation, the supernatant was loaded onto the column packed with HisPur Ni-NTA Resin (Fisher Scientific, Pittsburgh, PA, USA) and eluted with 100 mM MOPS buffer (pH 7.0) containing 300 mM NaCl and 250 mM imidazole. The purified proteins (10 μL) were loaded into 12% SDS-PAGE to check the qualty of purification (**Figure S1**).

General method for preparation of HN-ωTA in *E.coil* BL21(DE3) cells. Cells contain protein expression plasmids of HN-ωTA were grown in LB medium containing ampicillin (100mg/L) at 37°C 200rpm. When A_{600} reached about 0.8, 100 μM IPTG (final concentration) was added and the cultivation temperature was decreased to 18 °C for ~10 hours. After IPTG induction, the cells were harvested by centrifugation at 17,000g, 4°C, 20 min. The pellet was washed with MOPS buffer (100 mM, pH=7.0), frozen with liquid nitrogen and lyophilized. The obtained cell were stored at -20°C.

Enzyme activity assays. Conventional nitrogenase activity assays were performed as reported previously.[22-23] Assays were performed in 9.6 mL vials (septum-sealed) that contained 1 mL of anaerobic ATP-regeneration solution (100 mM MOPS, pH=7.0 6.7 mM $MgCl_2$, 30 mM

creatine phosphate, 5 mM ATP, 0.2 mg/mL creatine phosphokinase and 1.3 mg/mL bovine serum albumin). The assay required dithionite (DT) as the primary electron donor, a final concentration of 15 mM was used and a Fe:MoFe protein mole ratio of 16:1 was adopted (0.1 mg of MoFe protein per assay). The assay was performed at 30 °C. An NH_3 detection reagent was prepared by mixing MOPS buffer (pH=7.0, 100 mM, 100 mL), 2-mercaptoethanol (25 μL) and *ortho*-phthalaldehyde (270 mg dissolved in 5 mL ethanol) and storing in the dark. Following N_2 reduction experiments, 250 μL of reaction solution (containing NH_3 produced by MoFe protein) was mixed with 1000 μL of the NH_3 detection reagent and incubated at for 30 min in the dark. NH_3 was quantified by exciting the solutions at 410 nm and measuring their emission reading at 472 nm. All samples were quantified as triplicates. The activity was expressed as units (U) per mg MoFe protein, where 1 U was defined as 1 μmol NH_3 generated per min. The specific activity is 0.82 ± 0.03 U/mg MoFe protein.

The activity of AlaDH was measured by the rate of oxidation of NADH at 30°C as reported previously.[47] The decrease of absorbance change at 340 nm was recorded in an Evolution 260 Bio UV-visible spectrophotometer (Thermo Scientific, Waltham, MA). The reaction mixture contained 100mM MOPS (pH=7.0), 0.16mM NADH, AlaDH, 5 mM pyruvate and 100 mM NH_4Cl. The millimolar extinction coefficient of NADH (ε_{340}) was 6.2 $mM^{-1}cm^{-1}$. AlaDH activity was expressed as units (U) per mg AlaDH, where 1 U was defined as 1 μmol alanine generated (consuming 1 μmol NADH) per min. The specific activity of AlaDH is 191.5 ± 5.2 U/mg.

The activity of DI were determined at 30°C by measuring the absorbance change at 578 nm in 1 min.[42] The enzyme reactions were carried out in an anaerobic screw-cap IR quartz cuvette (Reflex Analytical Co., Ridgewood, NJ, USA) with a degassed 100 mM MOPS buffer (pH 7.0) containing 2 mM NADH. 100 μM reduced methyl viologen ($MV^{\cdot+}$) prepared by a rotating disc electrode was used as an electron donor. The decrease in A_{578} was detected during the reactions. Millimolar extinction coefficients (ε_{578}) for reduced $MV^{\cdot+}$ was 9.78 $mM^{-1}cm^{-1}$. DI activity was expressed as units (U) per mg DI, while 1 U was defined as 1 μmol NADH generated per min. As the generation of 1 mole NADH consumes 1 mole reduced $MV^{\cdot+}$, the concentration of generated NADH was determined by the consumption of reduced $MV^{\cdot+}$. The specific activity of DI is 4.14 ± 0.18 U/mg.

The activity of HN-ωTA were assayed by employing 4-phenyl-2-butanone (50 mM) as substrate at 30°C. Alanine (250 mM) was used as the source of exogenous amine. A typical sample was prepared using 10 mg of *E.coil* cells containing overexpressed HN-ωTA in MOPS buffer (pH=7, 100 mM, 1 mM pyridoxal 5'-phosphate). The generated 1-methyl-3-phenylpropylamine was determined by Agilent 5975C gas chromatography (GC) equipped with DB-5ms column and Triple-Axis Detector. In order to remove the generated pyruvate and recycle alanine, 150 mM NH_4Cl, 1 mM NAD^+ and 10U/mL AlaDH were combined. 150 mM glucose and 10U/mL glucose dehydrogenase were also combined for the NADH regeneration. HN-ωTA activity was expressed as units (U) per mg *E. coli* cell, while 1 U was defined as 1 μmol 1-methyl-3-phenylpropylamine generated per min. The apparent specific activity of ω-TA is 0.0052 ± 0.0002 U/mg dry *E. coli* cells.

Electrochemical methods. Electrochemical measurements were conducted using a CH Instrument model 660e potentiostat anaerobically at 30°C. The experiments were operated within custom-made septum-sealed H-shaped electrochemical cells, where a Nafion® 212 proton exchange membrane was used to compartmentalize the anodic and cathodic chamber. Toray carbon paper electrodes were cut and coated with paraffin wax to regulate their geometric surface area and to prevent corrosion upon contact with their electrical contacts. Platinum mesh was used as a counter electrode. SCE was used as a reference electrode for all of the electrochemical experiments.

The initial CV analysis was used to demonstrate the ability of cathode to act as the primary electron donor for the N_2 reduction catalyzed by nitrogenase and NADH regeneration catalyzed by DI, where MV^{2+} serves as an electron mediator between the electrode and both nitrogenase and DI. Cyclic voltammetric experiments were performed by sequentially adding the nitrogenase, DI and NAD^+. The electrode was allowed to stabilize by scanning the potential between -0.9 and -0.475v for 8 cycles with a scan rate of 5 mV/s.

Amperometric *i*-t analyses was performed using a bulk electrolysis configuration. The reactions were performed in an H-shaped dual-chamber bioelectrochemical reactor and the headspace of the reactor was filled with high purity nitrogen at 1 atm. Because the MV^{2+} has a formal redox potential of approximately -0.75 V vs SCE (saturated calomel electrode), the applied constant potential was selected to be -0.85 V vs SCE to ensure a sufficient overpotential to drive the reaction into the reduction of MV^{2+}. The current was recorded every 1 s. The experiments were performed at 30 °C in an anaerobic H-shaped cell with stirring in N_2 reduction compartment (3 mL, complete with the ATP-regeneration system), where the 0.16 U/mL nitrogenase (0.2 mg/mL of MoFe protein coupled with Fe protein at 1:16 ratio by mol) and the $MgCl_2$ concentration was 6.7 mM. 0.1 U/mL dry *E. coli* cells (20 mg/mL) was initially added as well. In the 1st injection, 0.18 U/mL AlaDH, 0.16 U/mL DI, 200 μM NAD^+ and 50 μM pyruvate was supplemented. In the 2nd injection, 2 mM 4-phenyl-2-butanone and 1% DMSO was supplemented.

Bioelectrosynthesis of chiral amine chemicals. The bioelectrocatalytic *in vitro* synthesis of chiral amine chemicals was performed in an H-shaped dual-chamber bioelectrochemical reactor at constant potential of -0.85 V vs SCE at 30 °C. The headspace of the reactor was filled with high purity N_2 at 1 atm. The pH value the bioelectrosynthetic reaction was set at 7.0 as all the enzymes used in this study, including nitrogenase, DI, AlaDH and HN-ωTA worked well at pH = 7.0.[8, 22, 42] The reaction mixture contained 100 mM MOPS buffer (pH=7.0), 6.7 mM $MgCl_2$, 30 mM creatine phosphate, 5 mM ATP, 0.2 mg/mL creatine phosphokinase, 1.3 mg/mL bovine serum albumin, 50 μM pyruvate, 200 μM NAD^+,

1mM PLP, 2 mM ketone substrate and 1% DMSO. The enzymes loading were 0.16 U/mL nitrogenase, 0.18 U/mL AlaDH, 0.16 U/mL DI, and 0.10 U/mL HN-ωTA. After 10 hours of reaction, the reaction was stopped by adding aqueous NaOH (20% v/v, 10N). As the dication form of methyl viologen is hardly soluble in such solvents,[48] the cathode chamber was open to oxidize the $MV^{\cdot+}$ to MV^{2+}. The final chiral amine products were extracted by using ethyl acetate. The organic phase was dried by Na_2SO_4. The concentration and the optical purity (% ee_p) of the produced amine chemicals were determined by GC. The current was recorded by a potentiostat (CHI660). The faradaic efficiency (FE) for the formation of different amines was calculated as follow.

$$\mathrm{FE} = \frac{9\mathrm{F}n}{\int_0^t Idt} \times 100\ \%$$

Where 9 is the number of electrons transferred for the formation of one molecule of amine (8 electrons for N_2 fixation,[22] 1 electron for the regeneration of NADH), F is the Faraday constant (96485C/mol), n is the moles of generated amine, I is the circuit current and t is the reaction time.

Analytical methods. The conversion of amines was measured by GC using an Agilent 5975C that equipped with DB-5MS column (30m × 0.25mm × 0.25μm) and Triple-Axis Detector. The chiral analysis of produced amines was performed by GC as well. After ethyl acetate extraction, the organic phase was dried over Na_2SO_4 and the extracted amines were derivatized to the trifluoroacetamides by adding 20-fold excess of trifluoroacetic anhydride.[49] After 5 min at room temperature and purging with nitrogen to remove excess anhydride, residual trifluoracetic acid, and solvent, the derivatized compounds were dissolved in 50 μL ethyl acetate and 0.5 μL of this solution was injected into a Hewlett Packard 6890 Series gas chromatograph equipped with an Agilent CP-Chirasil Dex-CB (25 m, 320 μm, 0.25 μm). The GC program parameters are listed in supporting information.

ASSOCIATED CONTENT

Supporting Information. This Supporting Information is available free of charge via the Internet at http://pubs.acs.org.

The amino acid sequences of protein, the SDS-PAGE gel of proteins, the optimization of nitrogenase concentration, the UPLC-MS characterization of generated alanine, the GC-MS characterization of generated 1-methyl-3-phenylpropylamine, the molecular structure of chiral amines obtained from upgraded N_2 fixation, GC analysis program, the strains, plasmids and primers used in this study (PDF)

AUTHOR INFORMATION

Corresponding Author

* Shelley D. Minteer: minteer@chem.utah.edu

ORCID

Hui Chen: 0000-0002-8944-0090

Shelley D. Minteer: 0000-0002-5788-2249

NOTE

The authors declare no competing financial interest.

ACKNOWLEDGMENTS

The authors would like to thank the National Science Foundation Center for Synthetic Organic Electrosynthesis for funding (CHE-1740656) and Fulcrum Bioscience for funding this research.

REFERENCES

(1) Wang, B.; Land, H.; Berglund, P. An efficient single-enzymatic cascade for asymmetric synthesis of chiral amines catalyzed by ω-transaminase. *Chem. Comm.* **2013,** 49, 161-163.

(2) Koszelewski, D.; Göritzer, M.; Clay, D.; Seisser, B.; Kroutil, W. Synthesis of optically active amines employing recombinant ω-transaminases in *E. coli* cells. *ChemCatChem* **2010,** 2, 73-77.

(3) Scheidt, T.; Land, H.; Anderson, M.; Chen, Y.; Berglund, P.; Yi, D.; Fessner, W. D. Fluorescence - Based Kinetic Assay for High-Throughput Discovery and Engineering of Stereoselective ω-Transaminases. *Adv. Synth. Catal.* 2015, 357, 1721-1731.

(4) Shin, J. S.; Kim, B. G. Asymmetric synthesis of chiral amines with ω-transaminase. *Biotechnol. Bioeng.* **1999,** 65, 206-211.

(5) Hoehne, M.; Kuehl, S.; Robins, K.; Bornscheuer, U. T. Efficient asymmetric synthesis of chiral amines by combining transaminase and pyruvate decarboxylase. *ChemBioChem* **2008,** 9, 363-365.

(6) Koszelewski, D.; Tauber, K.; Faber, K.; Kroutil, W. ω-Transaminases for the synthesis of non-racemic α-chiral primary amines. *Trends Biotechnol*. **2010,** 28, 324-332.

(7) Koszelewski, D.; Lavandera, I.; Clay, D.; Guebitz, G. M.; Rozzell, D.; Kroutil, W. Formal asymmetric biocatalytic reductive amination. *Angew. Chem. Int. Ed.* **2008,** 120, 9477-9480.

(8) Mutti, F. G.; Fuchs, C. S.; Pressnitz, D.; Sattler, J. H.; Kroutil, W. Stereoselectivity of four (R)-selective transaminases for the asymmetric amination of ketones. *Adv. Synth. Catal.* **2011,** 353, 3227-3233.

(9) Van Der Donk, W. A.; Zhao, H. Recent developments in pyridine nucleotide regeneration. *Curr. Opin. Biotechnol.* **2003,** 14, 421-426.

(10) Kim, Y. H.; Yoo, Y. J. Regeneration of the nicotinamide cofactor using a mediator-free electrochemical method with a tin oxide electrode. *Enzyme Microb. Technol.* **2009,** 44, 129-134.

(11) Ali, I.; Gill, A.; Omanovic, S. Direct electrochemical regeneration of the enzymatic cofactor 1, 4-NADH employing nano-patterned glassy carbon/Pt and glassy carbon/Ni electrodes. *Chem. Eng. J.* **2012,** 188, 173-180.

(12) Zhang, L.; Vila, N.; Kohring, G. W.; Walcarius, A.; Etienne, M. Covalent immobilization of (2, 2'-Bipyridyl)(Pentamethylcyclopentadienyl)-Rhodium complex on a porous carbon electrode for efficient electrocatalytic NADH regeneration. *ACS Catal.* **2017,** 7, 4386-4394.

(13) Freguia, S.; Virdis, B.; Harnisch, F.; Keller, J. Bioelectrochemical systems: Microbial versus enzymatic catalysis. *Electrochim. Acta* **2012,** 82, 165-174.

(14) Wu, R.; Zhu, Z. Self-powered enzymatic electrosynthesis of l-3, 4-Dihydroxyphenylalanine in a hybrid bioelectrochemical system. *ACS Sustain. Chem. Eng.* **2018,** 6, 12593-12597.

(15) Kuk, S. K.; Singh, R. K.; Nam, D. H.; Singh, R.; Lee, J. K.; Park, C. B. Photoelectrochemical reduction of carbon dioxide to methanol through a highly efficient enzyme cascade. *Angew. Chem. Int. Ed.* **2017,** 56, 3827-3832.

(16) Dominguez-Benetton, X.; Srikanth, S.; Satyawali, Y.; Vanbroekhoven, K.; Pant, D. Enzymatic electrosynthesis: an

overview on the progress in enzyme-electrodes for the production of electricity, fuels and chemicals. *J. Microb. Biochem. Technol.* **2013,** 6, 7.

(17) Alkotaini, B.; Abdellaoui, S.; Hasan, K.; Grattieri, M.; Quah, T.; Cai, R.; Yuan, M.; Minteer, S. D. Sustainable bioelectrosynthesis of the bioplastic polyhydroxybutyrate: Overcoming substrate requirement for NADH regeneration. *ACS Sustain. Chem. Eng.* **2018,** 6, 4909-4915.

(18) Chen, X.; Cao, Y.; Li, F.; Tian, Y.; Song, H. Enzyme-assisted microbial electrosynthesis of poly (3-hydroxybutyrate) via CO_2 bioreduction by engineered *Ralstonia eutropha*. *ACS Catal.* **2018,** 8, 4429-4437.

(19) Märkle, W.; Lütz, S. Electroenzymatic strategies for deracemization, stereoinversion and asymmetric synthesis of amino acids. *Electrochim. Acta.* **2008,** 53, 3175-3180.

(20) Yuan, R.; Watanabe, S.; Kuwabata, S.; Yoneyama, H. Asymmetric electroreduction of ketone and aldehyde derivatives to the corresponding alcohols using alcohol dehydrogenase as an electrocatalyst. *J. Org. Chem.* **1997,** 62, 2494-2499.

(21) Weckbecker, A.; Gröger, H.; Hummel, W., Regeneration of nicotinamide coenzymes: principles and applications for the synthesis of chiral compounds. *In Biosystems Engineering I*, Springer: Berlin **2010**; pp 195-242.

(22) Milton, R. D.; Cai, R.; Abdellaoui, S.; Leech, D.; De Lacey, A. L.; Pita, M.; Minteer, S. D. Bioelectrochemical Haber-Bosch Process: An Ammonia-producing H_2/N_2 fuel cell. *Angew. Chem. Int. Ed.* **2017,** 56, 2680-2683.

(23) Milton, R. D.; Abdellaoui, S.; Khadka, N.; Dean, D. R.; Leech, D.; Seefeldt, L. C.; Minteer, S. D. Nitrogenase bioelectrocatalysis: heterogeneous ammonia and hydrogen production by MoFe protein. *Energy Environ. Sci.* **2016,** 9, 2550-2554.

(24) Howard, J. B.; Rees, D. C. Structural basis of biological nitrogen fixation. *Chem. Rev.* **1996,** 96, 2965-2982.

(25) Rees, D. C.; Tezcan, F. A.; Haynes, C. A.; Walton, M. Y.; Andrade, S.; Einsle, O.; Howard, J. B. Structural basis of biological nitrogen fixation. *Philos. Trans. Royal Soc. A* **2005,** 363, 971-984.

(26) Foster, S. L.; Bakovic, S. I. P.; Duda, R. D.; Maheshwari, S.; Milton, R. D.; Minteer, S. D.; Janik, M. J.; Renner, J. N.; Greenlee, L. F. Catalysts for nitrogen reduction to ammonia. *Nat. Catal.* **2018,** 1, 490.

(27) Smith, B. E. Nitrogenase reveals its inner secrets. *Science* **2002,** 297, 1654-1655.

(28) Balaraman, E.; Srimani, D.; Diskin-Posner, Y.; Milstein, D. Direct synthesis of secondary amines from alcohols and ammonia catalyzed by a ruthenium pincer complex. *Catal. Lett.* **2015,** 145, 139-144.

(29) Shin, J. S.; Kim, B. G. Substrate inhibition mode of ω-transaminase from *Vibrio fluvialis* JS17 is dependent on the chirality of substrate. *Biotechnol. Bioeng.* **2002,** 77, 832-837.

(30) Yun, H.; Hwang, B.-Y.; Lee, J.-H.; Kim, B.-G. Use of enrichment culture for directed evolution of the *Vibrio fluvialis* JS17 ω-transaminase, which is resistant to product inhibition by aliphatic ketones. *Appl. Environ. Microbiol.* **2005,** 71, 4220-4224.

(31) Badalyan, A.; Yang, Z.; Seefeldt, L. C. A Voltammetric study of nitrogenase catalysis using electron transfer mediators. *ACS Catal.* **2019,** 9, 1366-1372.

(32) Li, H.; Zhu, D.; Hyatt, B. A.; Malik, F. M.; Biehl, E. R.; Hua, L. Cloning, protein sequence clarification, and substrate specificity of a leucine dehydrogenase from *Bacillus sphaericus* ATCC4525. *Appl. Biochem. Biotechnol.* **2009,** 158, 343-351.

(33) Brunhuber, N. M.; Thoden, J. B.; Blanchard, J. S.; Vanhooke, J. L. *Rhodococcus* L-phenylalanine dehydrogenase: kinetics, mechanism, and structural basis for catalytic specifity. *Biochemistry* **2000,** 39, 9174-9187.

(34) Navarrete, R. M.; Vara, J. A.; Hutchinson, C. R. Purification of an inducible L-valine dehydrogenase of *Streptomyces coelicolor* A3 (2). *Microbiology* **1990,** 136, 273-281.

(35) Campbell, E.; Meredith, M.; Minteer, S. D.; Banta, S. Enzymatic biofuel cells utilizing a biomimetic cofactor. *Chem. Comm.* **2012,** 48, 1898-1900.

(36) Sanfilippo, C.; Paternò, A. A.; Patti, A. Resolution of racemic amines via lipase-catalyzed benzoylation: Chemoenzymatic synthesis of the pharmacologically active isomers of labetalol. *Mol. Catal.* **2018,** 449, 79-84.

(37) Ye, L. J.; Toh, H. H.; Yang, Y.; Adams, J. P.; Snajdrova, R.; Li, Z. Engineering of amine dehydrogenase for asymmetric reductive amination of ketone by evolving *Rhodococcus* phenylalanine dehydrogenase. *ACS Catal.* **2015,** 5, 1119-1122.

(38) Huang, L.; Liu, J.; Shan, W.; Liu, B.; Shi, A.; Li, X. The asymmetric synthesis of (R, R)-formoterol via transfer hydrogenation with polyethylene glycol bound Rh catalyst in PEG2000 and water. *Chirality* **2010,** 22, 206-211.

(39) Cavalluzzi, M. M.; Catalano, A.; Bruno, C.; Lovece, A.; Carocci, A.; Corbo, F.; Franchini, C.; Lentini, G.; Tortorella, V. Synthesis of (R)-,(S)-, and (RS)-hydroxymethylmexiletine, one of the major metabolites of mexiletine. *Tetrahedron: Asymmetry* **2007,** 18, 2409-2417.

(40) González-Sabín, J.; Gotor, V.; Rebolledo, F. CALB-catalyzed resolution of some pharmacologically interesting β–substituted isopropylamines. *Tetrahedron: Asymmetry* **2002,** 13, 1315-1320.

(41) Yoshida, A.; Freese, E., l-Alanine dehydrogenase (*Bacillus subtilis*). *In Methods in enzymology*, Elsevier: **1970;** Vol. 17, pp 176-181.

(42) Chen, H.; Huang, R.; Kim, E. J.; Zhang, Y. H. P. J. Building a thermostable metabolon for facilitating coenzyme transport and *in vitro* hydrogen production at elevated temperature. *ChemSusChem* **2018,** 11, 3120-3130.

(43) Wilhelm, E.; Battino, R.; Wilcock, R. J. Low-pressure solubility of gases in liquid water. *Chem. Rev.* **1977,** 77, 219-262.

(44) Hickey, D. P.; Lim, K.; Cai, R.; Patterson, A. R.; Yuan, M.; Sahin, S.; Abdellaoui, S.; Minteer, S. D. Pyrene hydrogel for promoting direct bioelectrochemistry: ATP-independent electroenzymatic reduction of N_2. *Chem. Sci.* **2018,** 9, 5172-5177.

(45) Christiansen, J.; Goodwin, P. J.; Lanzilotta, W. N.; Seefeldt, L. C.; Dean, D. R. Catalytic and biophysical properties of a nitrogenase apo-MoFe protein produced by an nifB-deletion mutant of *Azotobacter vinelandii*. *Biochemistry* **1998,** 37, 12611-12623.

(46) You, C.; Zhang, X.-Z.; Zhang, Y.-H. P. Simple cloning via direct transformation of PCR product (DNA Multimer) to *Escherichia coli* and *Bacillus subtilis*. *Appl. Environ. Microbiol.* **2012,** 78, 1593-1595.

(47) Yoshida, A.; Freese, E. Purification and chemical characterization of alanine dehydrogenase of *Bacillus subtilis*. *Biochim. Biophys. Acta.* **1964,** 92, 33-43.

(48) Takuma, K.; Sonoda, T.; Kobayashi, H. Redox behavior of methylviologen cation radical incorporated into a hydrophobic organic phase by lipophilic stable anions. *Chem. Lett.* **1984,** 13, 243-246.

(49) Schätzle, S.; Steffen-Munsberg, F.; Thontowi, A.; Höhne, M.; Robins, K.; Bornscheuer, U. T. Enzymatic asymmetric synthesis of enantiomerically pure aliphatic, aromatic and arylaliphatic amines with (R)-selective amine transaminases. *Adv. Synth. Catal.* **2011,** 353, 2439-2445.

Authors are required to submit a graphic entry for the Table of Contents (TOC) that, in conjunction with the manuscript title, should give the reader a representative idea of one of the following: A key structure, reaction, equation, concept, or theorem, etc., that is discussed in the manuscript. Consult the journal's Instructions for Authors for TOC graphic specifications.